

# Small Coil MRI of the Nipple-Areola Complex and Retroareolar Breast

Mariá Soledad Muñoz, MD; Maria Laura Alvares, MD; Daniela Muñoz Tisera, MD; Marcelo Elias Muñoz, MD

Imaging assessment of the nipple-areola complex and the retroareolar breast includes diagnostic mammography and targeted ultrasound as first-line imaging techniques, with magnetic resonance imaging (MRI) serving as a complementary alternative that nonetheless often leads to inconclusive results.<sup>1-6</sup>

In MRI, the sequences and coils, regardless of their brand or design, lack the necessary resolution for effective analysis of the ductal system, its contents, and the surrounding parenchyma.<sup>7</sup>

In this article, we present a practical application of focused, magnified, high-resolution MRI with contrast using commercially available small coils.<sup>8</sup> This approach is equivalent to the microfocus, spot magnification view traditionally used in diagnostic mammography. In this regard, we must discuss pioneering publications dealing with the efficacy of small coils in high-resolution analysis of different kinds of breast lesions.<sup>9</sup>

The small coil is used mainly to detect lesions not seen on standard imaging evaluation, to confirm positive findings with conventional

techniques (mammography, ultrasound, MRI), and to present them in an accessible way for surgeons and the pathologists.<sup>10</sup>

## Breast MRI with Small Coil Technique

The exam is performed on a 1.5T MRI scanner with a small surface coil focused on the areola instead of a conventional bilateral coil.

Owing to its design and dimensions, the small coil allows for ventral and lateral decubitus explorations according to the patient's anatomical needs. The coil's high performance facilitates the study of the areola and the underlying parenchyma up to a depth of 6-7 cm from the nipple, including divisions of the ducts up to the fourth grade.<sup>11</sup>

The protocol consists of T2 3D TSE (3D turbo spin echo), T1 3D FFE (3D fast field echo) and T1 3D FFE EPI (3D fast field echo-echo planar), fat-saturated sequences with and without contrast and obtained only in the axial plane. The geometry and contrast of these sequences are shown in Table 1.

The first sequence (T2 SPAIR) demonstrates ducts with serous or serosanguinous content. The second (T1 SPIR) and the third sequence (T1 SPIR-EPI) mainly detect blood products and are used before contrast administration.

After contrast injection, the second and third sequences are repeated, with the fourth sequence concluding the imaging. The fourth sequence (T1 SPIR FOV 150 mm) is optional; it has a lower resolution but a larger FOV, and provides information regarding the topography, lesion extension, and any additional findings.

Only fat-saturation sequences are applied, not only because gadolinium is used but also because the resolution provided by the coil does not require the presence of fat to identify typical lesions in this breast segment. The only artifacts are those generated by patient movement that can occur.

This is predominately a high-resolution morphological study without dynamic curves because the small coil provides images with average acquisition times of two to three minutes. The enhancement hierarchy could be visually estimated.

Regarding FOV, the software adjusts the matrix, providing  $0.49 \times 0.49$  mm pixels with 0.7 mm slices in T2 (TSE) and  $0.23 \times 0.23$  mm pixels with 0.6 mm slices in T1 (FF3D), with a resolution eight times higher than that of a conventional breast coil. This software also builds nonisotropic voxels that allow reconstruction in MIP (maximum intensity projection) and 3D volume rendering in

**Table 1. Contrast and geometry of sequences**

SEQUENCE	(1) T2 SPAIR	(2) T1 SPIR	(3) T1 SPIR-EPI	(4) T1 SPIR FOV 150 MM
Parameter	3D TSE	3D FFE	3D FFE	3D FFE
TE (ms)	235	8.7	7	8.7
TR (ms)	2000	43	35	43
Flip angle (°)	90	50	50	50
Reconstructed voxel size (mm)	0.49 x 0.49 x 0.7	0.23 x 0.23 x 0.6	0.22 x 0.22 x 1	0.23 x 0.23 x 2
Scan Time (min)	3.50 (2 NEX)	3.15 (1 NEX)	1.12 (2 NEX)	2.41 (1 NEX)
FOV (mm)	70	80	80	150
Philips Multiva 1.5T with dStream Microscopy coil® - Philips 4.7 cm diameter				
(1) T2 SPAIR, spectral attenuated inversion recovery (3D turbo spin echo)				
(2) T1 SPIR, spectral pre-saturation with inversion recovery (3D fast field echo)				
(3) T1 SPIR-EPI (3D fast field echo + echoplanar)				
(4) T1 SPIR FOV 150 (3D fast field echo with 150 mm field of view)				

the most representative planes (axial and sagittal) and video editing in three planes.<sup>12</sup>

### Imaging Findings

The resolution provided by the small coil represents the anatomy of the central major ducts to detect its signal (serous, sanguineous, and mixed) and the presence of filling defects. This high resolution allows detailed analysis of enhancements of the paramagnetic contrast inside the ducts and on their walls, as well as of masses and non-masses in the surrounding parenchyma.

The protocol is primarily used to evaluate patients with clinically significant nipple discharge, palpable findings in an inverted or retracted nipple, and Paget disease.

### Clinically Significant Nipple Discharge

Nipple discharge is the third-most common reason for clinical evaluation after mastodynia and palpable lump(s). The most common breast entities related to clinically significant nipple discharge are intraductal papilloma (40-70% of cases) and other benign causes.

Less frequent, but more relevant and concerning, is a malignant lesion (more commonly associated with bloody nipple discharge) that may be occult on mammography and ultrasound, such as in situ ductal carcinoma (DCIS).<sup>13,14</sup>

### Papilloma

Papillomas are classified into central, peripheral, and intracystic types and categorized as single or multiple. Central papillomas originate outside the terminal ductal-lobular unit and are generally solitary, whereas peripheral types tend to occur in multiples, owing to their origin in the terminal duct-lobular units.<sup>15</sup>

On mammograms papillomas are usually < 10 mm, circular/oval masses, with or without associated calcifications, which can be either coarse or crushed stone-like.<sup>15</sup>

The ultrasound appearance of intraductal papilloma is a solid, vascularized nodule located within a single, dilated duct in the subareolar area. The presence of a circumscribed margin does not distinguish benign from malignant papillary lesions.<sup>16</sup>

With the small coil, central papillomas appear as measurable, solid, filling defects in a major central duct

with or without gadolinium enhancement and with the most prominent ectasia in the proximal segment of the duct with varying MRI signal characteristics on T1 and T2, depending on the serous, proteinaceous, or hemorrhagic content (Figure 1, 2).<sup>17</sup>

Papillomas are characterized as single masses of different sizes and morphologies (node, bar-shaped, bifurcated, coral-like; Figure 3).

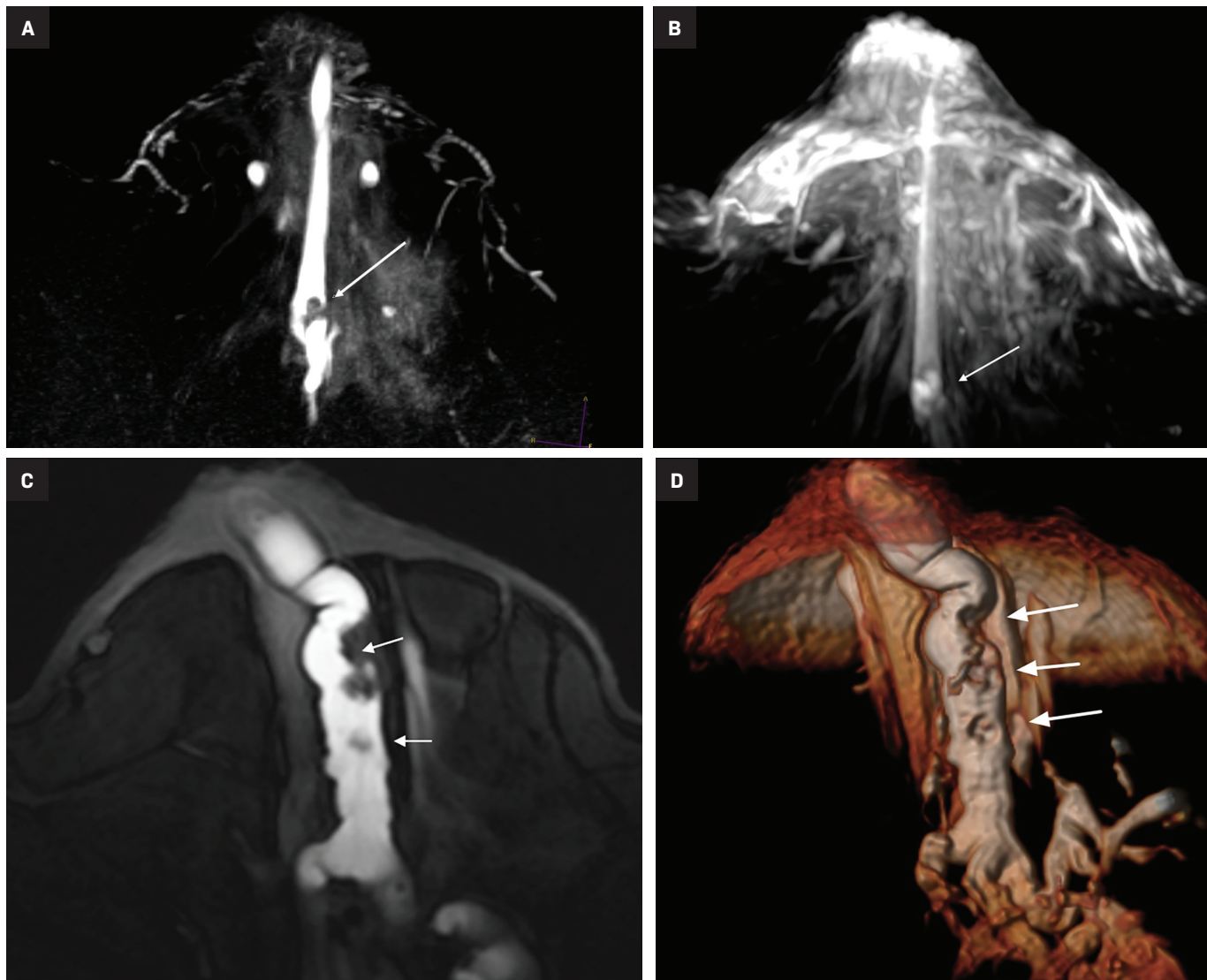
Multiple papillomas (10 percent of intraductal papillomas) are often deeper, more peripheral, and occur bilaterally; they are related to hyperplasia, atypia, adenosis, and sclerosing lesions. They appear on MRI as random enhancing small masses not always associated with ectatic ducts. Single papillomas are rarely associated with cancer (1.3%), but multiple papillomas confer a greater risk of cancer than a single papilloma.<sup>18,19,20</sup>

Intracystic papillomas (Figure 4) are rare (1%) and frequently occur in multiples. Differential diagnosis between intracystic papillomas and intracystic papillary carcinoma is difficult preoperatively.

### Other Benign Entities

There are other more diffuse, nonspecific, benign entities that

**Figure 1.** Central single papilloma. (A) Axial MIP T2 showing an ectatic central duct with bright serous signal intensity and filling defect (arrow). (B) Axial MIP T1 with gadolinium, showing an enhancing mass. Central multiple papillomas: (C) Axial MIP T2 showing an ectatic and tortuous central duct with serous signal intensity with filling defects (arrows); (D) Volume rendering.



allow more expectant management, including simple ductal ectasia, galactoceles (Figure 5), and fibrocystic mastopathies (Figure 6).

Normal milk ducts have longitudinal folds that disappear when the duct is distended by accumulation of fluid, cells, tumor, and detritus.<sup>21</sup> Small coil MRI readily demonstrates distended major lactiferous ducts. Given this, the more appropriate descriptive term is “ductal ectasia” instead of “dilated duct,” as the former refers to a measurement that originated and was used

in ultrasound imaging, within a range 1.0–4.4 mm.<sup>22</sup>

Depending on degree of distention and their contents, ectatic ducts can appear as filiform structures, tubular formations, or coarse cystic conglomerates in their most chronic stages. Ductal ectasia is usually an asymptomatic and nonspecific finding, but it may present with nipple discharge and is a frequent finding on ultrasound. MRI in simple ductal ectasia reveals uniformly distended ducts with fluid or serosanguineous intensity signal with normal caliber,

not distorted, with or without sub-millimeter filling defects and without wall enhancement. MRI with small coils also helps to precisely locate the compromised segment or quadrant if surgery is required.

### Breast Cancer

Breast cancer may clinically manifest with nipple inversion or retraction, a size increase and/or asymmetry on areolar palpation, as in Paget disease, or with significant nipple discharge as the only finding.

**Figure 2.** Papilloma at the nipple base. (A) Axial MIP T2, ectatic tortuous central duct with serous signal intensity and filling defect. (B) Volume rendering. (C) MIP T1 with contrast enhancing mass. Note: The tortuous segment of the duct at the base of the ampullary segment is a normal anatomical finding (small arrow in A, B).

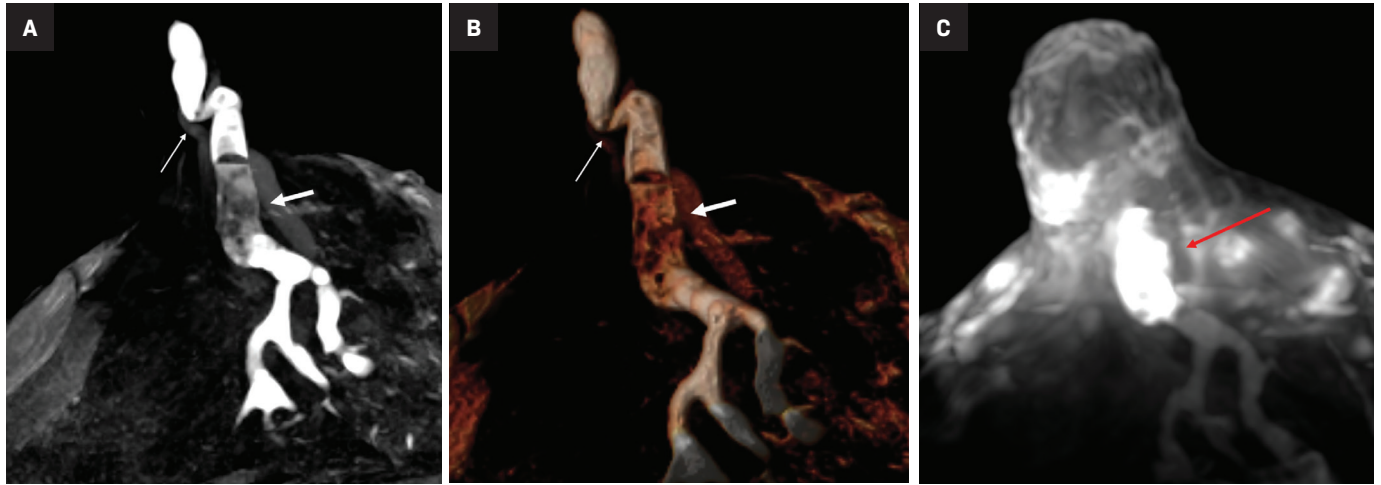
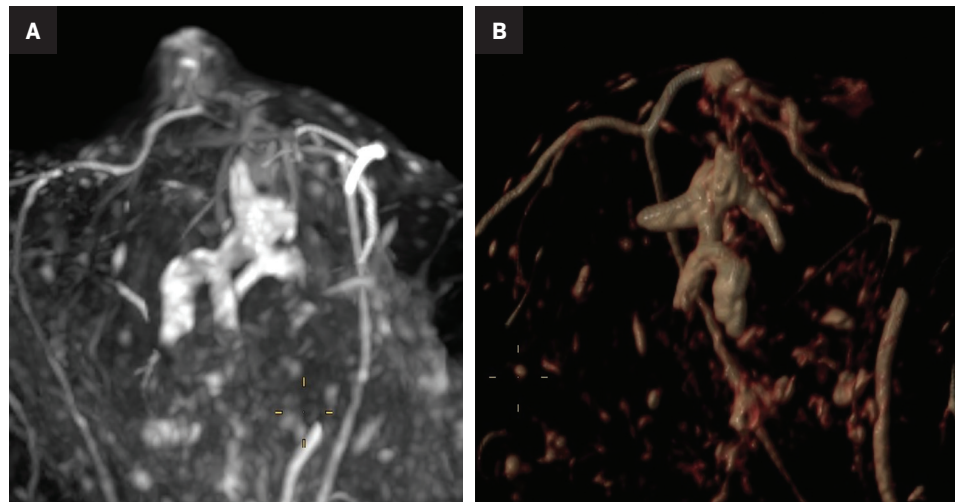


**Figure 3.** Coral-shaped papilloma enhancing on postcontrast T1 MIP. (A) Confluent multiple bars on MIP reconstruction and (B) volume-rendered reconstruction.



One subtype of breast cancer originating from the major lactiferous ducts presents with serous or bloody nipple discharge with a tumor growth pattern showing a mixture of papillary/micropapillary and/or cribriform growth without necrosis. No calcifications are expected on mammography in these cases, because, as Tabar indicates, “the nipple discharge prevents the long-term fluid stagnation within the duct”.<sup>23,24,25</sup>

As an initial exam, breast ultrasound can be effective for the detection of invasive carcinomas and certain types of DCIS, including intraductal papilloma with DCIS or

intraductal papillary carcinoma, which appear as masses. However, ultrasound may not be effective in detecting DCIS that manifests only with nipple discharge.

With small coil MRI, the micropapillary and cribriform growth patterns appear in discontinuous patches toward the nipple as non-mass-like regions of contrast enhancement, often in clustered rings, branching in an increasing number of abnormal ducts (neoductogenesis)<sup>25,26</sup>, with little or no contrast washout for 5-10 minutes.

Detected by MRI, these features allow for more accurate determination of their extent and anatomic location better than ultrasound, which is

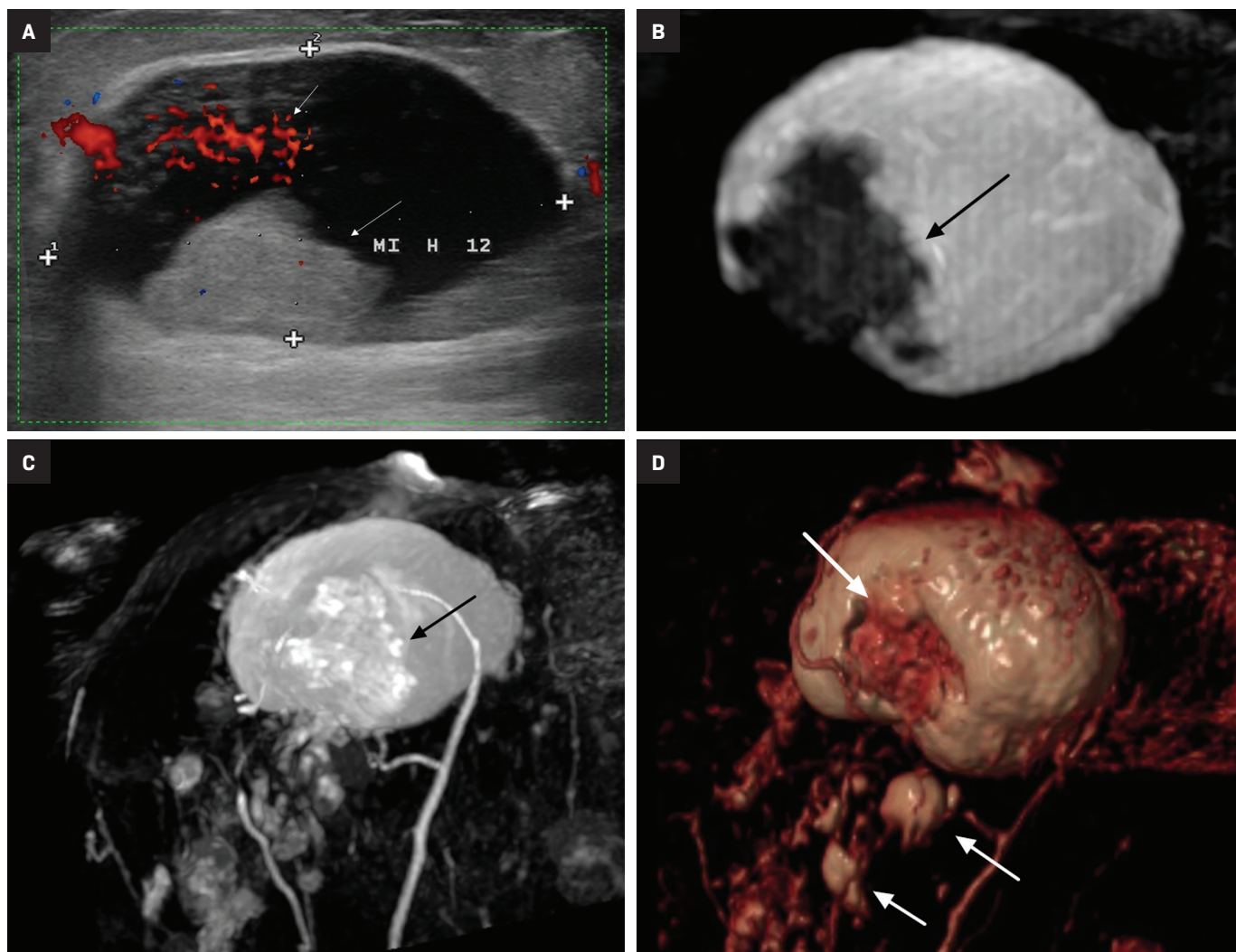
known to underestimate the extent of DCIS.<sup>27,28</sup> MRI with small coils better represents segmental distribution; ie, triangular on maximum intensity projections and pyramidal on 3D volume rendering (Figures 7, 8). This finding supports previously published data that confirmed the high positive predictive value for a malignant lesion when encountering the clustered ring enhancement pattern and segmental disposition.<sup>29,30</sup>

### Palpable Lesions with Inverted or Retracted Nipples

Small coil image findings may be conclusive in these clinical situations;



**Figure 4.** Giant intracystic papilloma presenting as a palpable mass. (A) Ultrasound of complex cystic mass with peripheral blood vessels along the solid component (arrows). (B) MIP T2 of cyst with filling defect from a frond-like mass (arrow). (C) Postcontrast T1 MIP shows the enhancing intracystic mass (black arrow) and small satellite masses. (D) Volume rendering of the same lesion with small satellite masses (white arrows).



they are primarily used to detect and characterize masses, to associate the retracted nipple with chronically diseased ducts, or to assess the need for surgical exploration (Figures 9, 10).

### Paget Disease

Once a lesion has been confirmed, either by mammography or ultrasound breast, MRI should also be performed, as the modality offers a detailed exploration of the central cone of the breast (Figure 11) to search for an underlying cancer.<sup>31</sup>

### Conclusion

MRI with small coils can provide a high-resolution targeted study (similar to diagnostic spot-magnified mammography) that can serve as an adjunct to standard techniques for evaluation of the nipple-areola complex and retroareolar breast.

### References

- 1) Bahl M, Gadd M, Lehman C. Diagnostic utility of MRI after negative or inconclusive mammography for the evaluation of pathologic nipple discharge. *AJR* 2017; 209:1404–1410.
- 2) Berger N, Luparia A, Di Leo G, et al. Diagnostic Performance of MRI versus galactography in women with pathologic nipple discharge: A systematic review and meta-analysis. *AJR* 2017; 209:465–471.
- 3) Sarica O, Ozturk E, Demirkurek H, Uluc F. Comparison of ductoscopy, galactography, and imaging modalities for the evaluation of intraductal lesions: A critical review. *Breast Care*. 2013; 8:348–354.
- 4) Srinivasan A, Nia E, Gupta M, Sun J, Leung J. Retrospective statistical analysis on the diagnostic value of ductography based on lesion pathology in patients presenting with nipple discharge. *The Breast Journal* 2019; 25:585–589.
- 5) Schedule K, Schnitzer A, Krammer J, Kaiser C, Schönberg S.O, Wasser K. Value of galactography for the diagnostic work-up of pathological nipple discharge in multimodal breast diagnostics. *Radiologie*. 2014. 54:160–166.

**Figure 5.** Galactocele. MIP T2 of ectatic ducts with large cystic dilatation (Inset: Volume-rendered reconstruction). (B) Ductal ectasia: MIP T2, ectatic ducts with serous signal intensity, no filling defects (Inset: volume-rendered reconstruction).

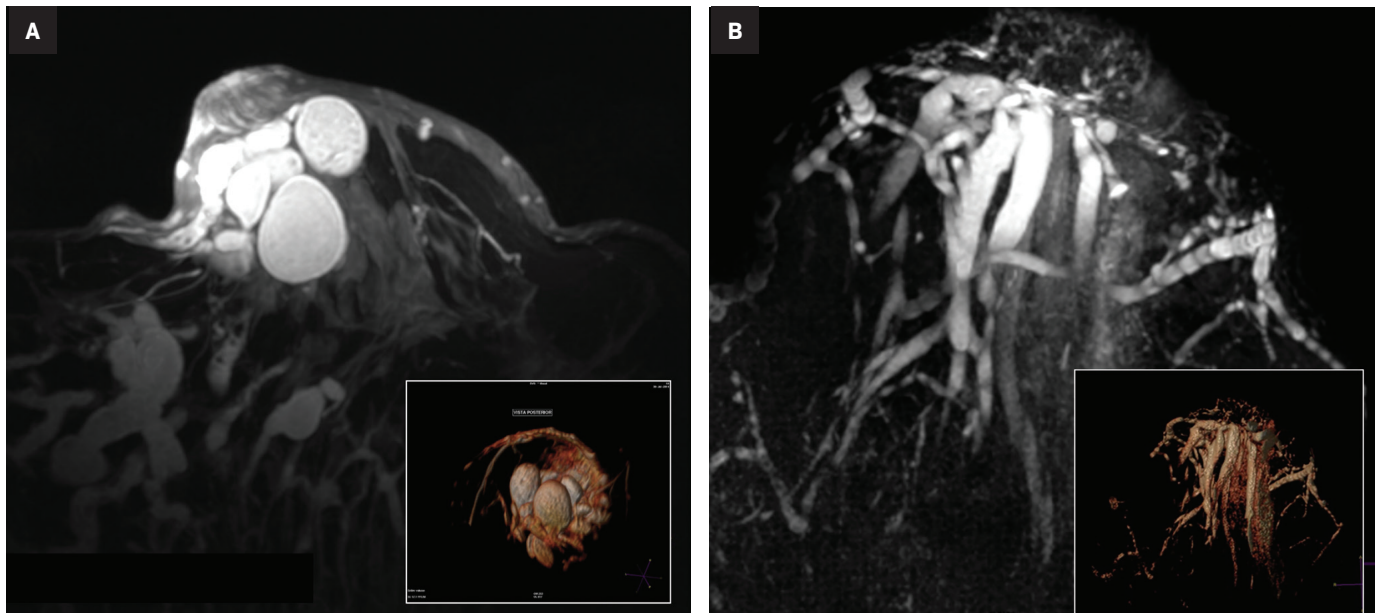
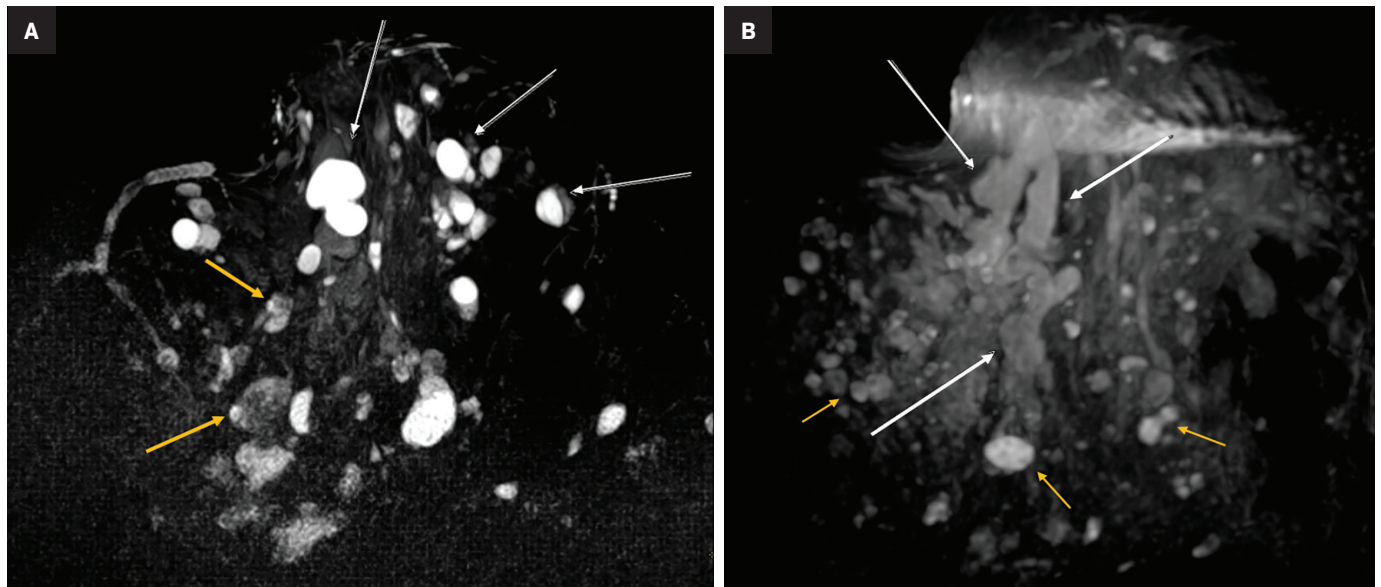


**Figure 6.** Fibrocystic mastopathy, mixed pattern with small nodules and cysts. (A) MIP T2 of cysts (white arrows) interposed with nodules (yellow arrows). (B) MIP T1 with gadolinium showing multiple small nodules (yellow arrows) along with central and peripheral ductal ectasia (white arrows).



6) Morrogh M, Park A, Elkin E.B, King T.A. Lessons learned from 416 cases of nipple discharge of the breast. *Am J Surg.* 2010; 200:73–80.

7) Kurihara Y. Microscopy coils provide SNR to resolve smallest anatomy. <http://clinical.netforum.healthcare.philips.com/global/Explore/Best-Practices>.

8) Kanemaki Y, Kurihara Y, Okamoto K, Nakajima Y, Fukuda M, Maeda I, et al. MR mammary ductography using a microscopy coil for assessment of intraductal lesions. *AJR.* 2004; 182:1340–1342.

9) Kanemaki Y, Kurihara Y, et al. Ductal carcinoma in situ: correlations between high-resolution magnetic resonance imaging and histopathology. *Radiat Med.* 2007; 25:1–7.

10) Zacharioudakis K, Kontoulis T, Vella J. Can we see what is invisible? The role of MRI in the evaluation and management of patients with pathological nipple discharge. *Breast Canc Res Treatm.* 2019; 178(1):115–120.

11) Ohuchi N, Abe R, Takahashi T, Tezuka F. Origin and extension of intraductal papillomas of the breast: a three-dimensional

reconstruction study. *Breast Cancer Res Treat.* 1984;4(2):117–28.

12) Simpfendorfer T, Li Z, Gasch C, et al. Three-dimensional reconstruction of preoperative imaging improves surgical success in laparoscopy. *J Laparoend Adv Surg Techn.* 2017; 27(2):181–185.

13) Lippa N, Hurtevent-Labrot G, Ferron S, Boissarie-Lacroix M. Nipple discharge: The role of imaging. *Diagn Intervent Imag.* 2015; 96(10):1017–1032.



**Figure 7.** Carcinoma presenting with bloody nipple discharge, negative ultrasound. (A) T1 with gadolinium, lateral focal non-mass enhancement (yellow arrow) (Inset: T1 without contrast, with bright hemorrhagic signal intensity in ectatic central ducts, white arrow). (B) Volume rendering (Inset: histopathology of papillary and cribriform carcinoma).

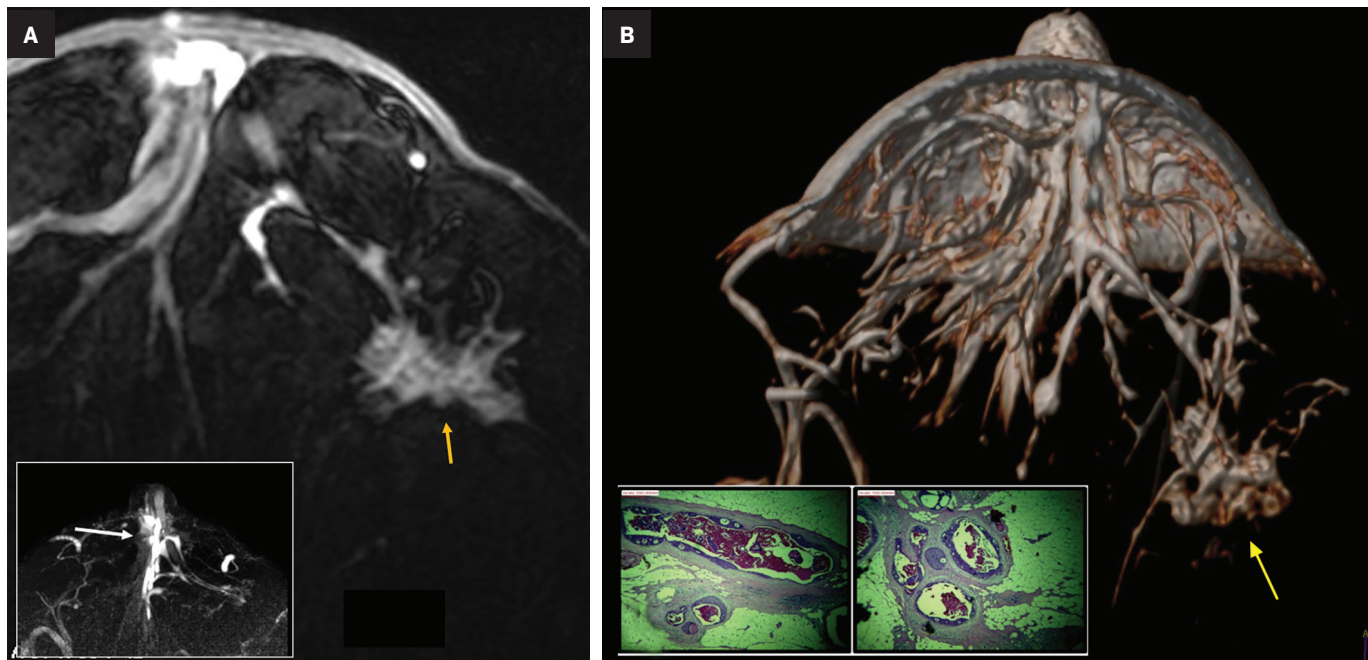


**Figure 8.** Carcinoma presenting with bloody nipple discharge. (A) MIP T1 with gadolinium, central duct with bright hemorrhagic signal intensity (yellow arrow) and non-mass enhancement in conglomerated rings (white arrows). (B) Volume rendering showing thickened walls in the central duct (yellow arrow) and conglomerated rings branching in ducts (white arrows). (C) Conglomerated rings: hypointense centers (yellow arrows) represent ducts filled by malignant proliferation and bright rings (red arrows) represent neo-angiogenesis in the stroma enhanced with gadolinium.

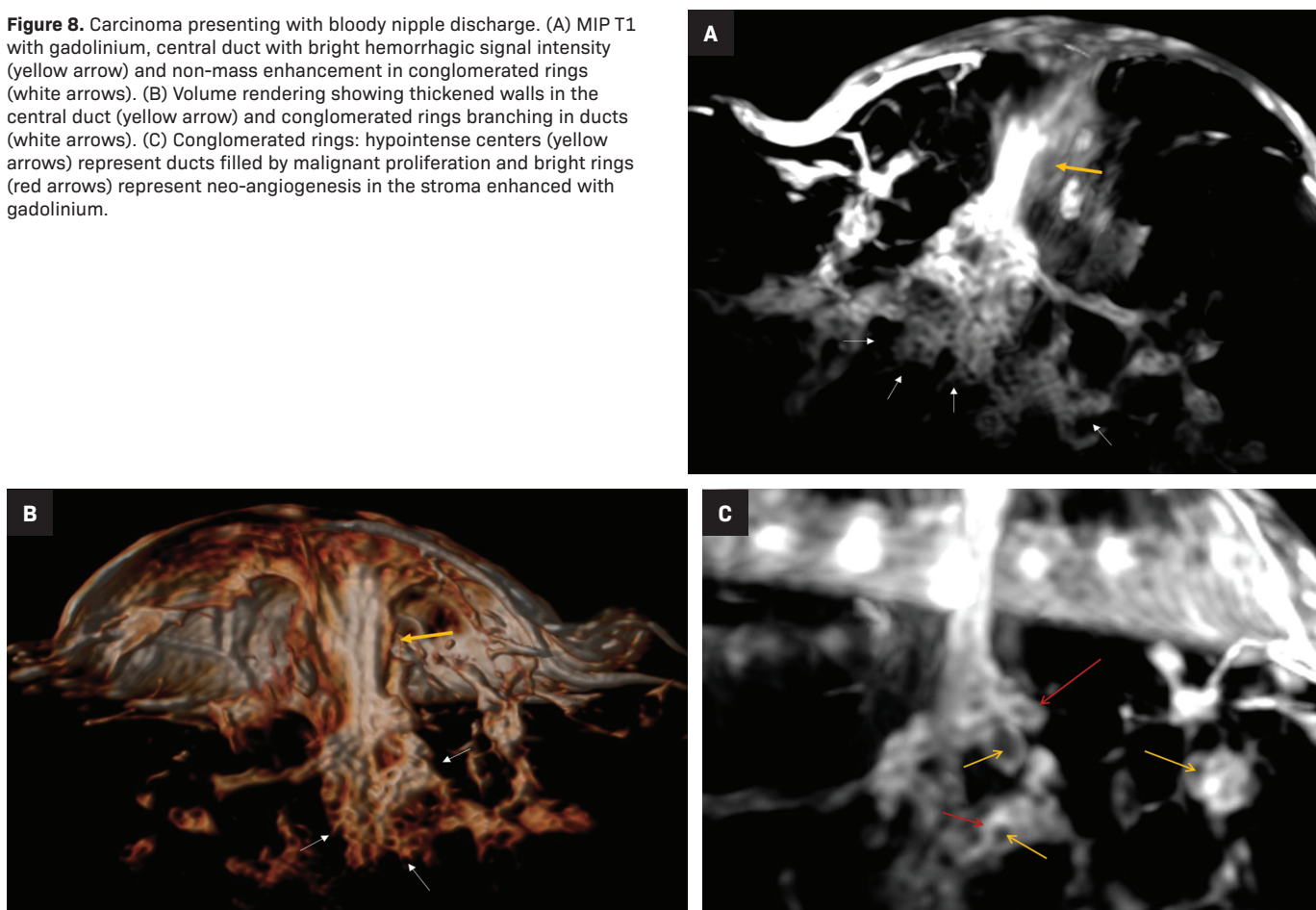


**Figure 9.** Palpable findings. (A) Ductal carcinoma: T1 with gadolinium, highly vascular, spiculated mass (inset: volume rendering). (B) Nipple adenoma: T1 with gadolinium, enhancing circumscribed lymph node (Inset: ultrasound showing nipple enlarged by a solid, vascular mass).

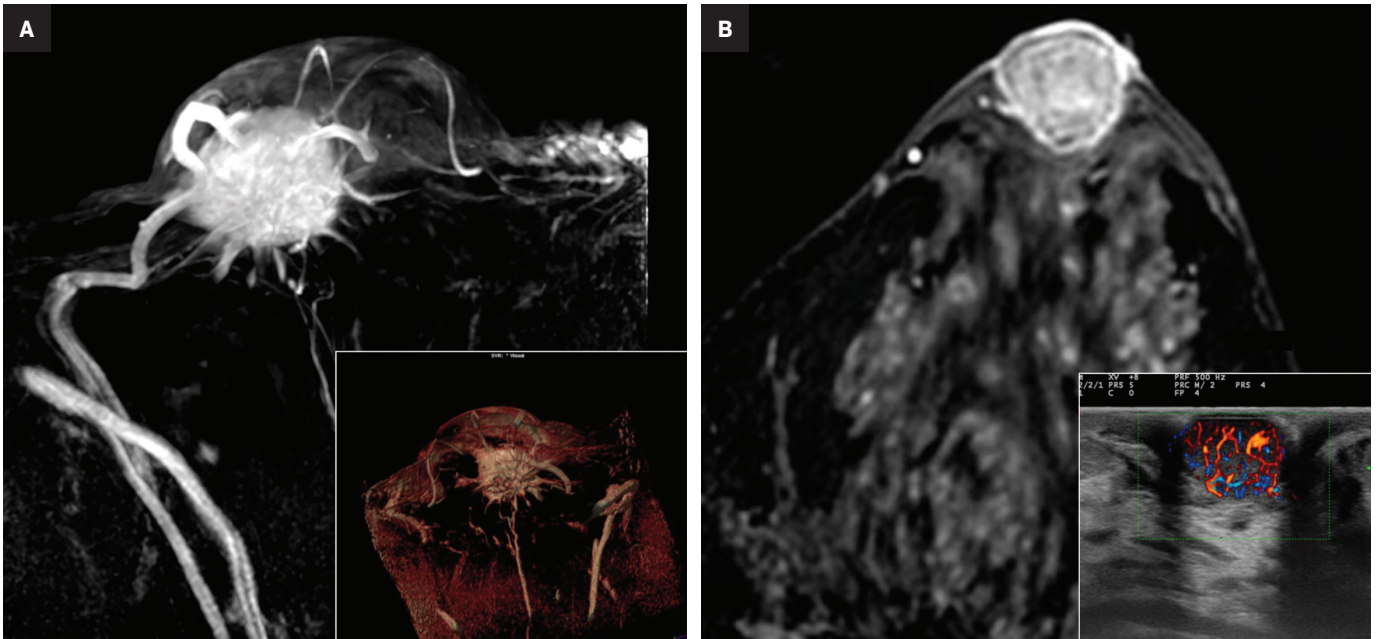


**Figure 10.** Retracted nipple. (A) Mammogram with subareolar distortion and retracted nipple (white arrow). (B) T1 with gadolinium, irregular spiculated mass (white arrow) with a thick retro-areolar band (yellow arrow). (C) Volume rendering of a classic lobular carcinoma.

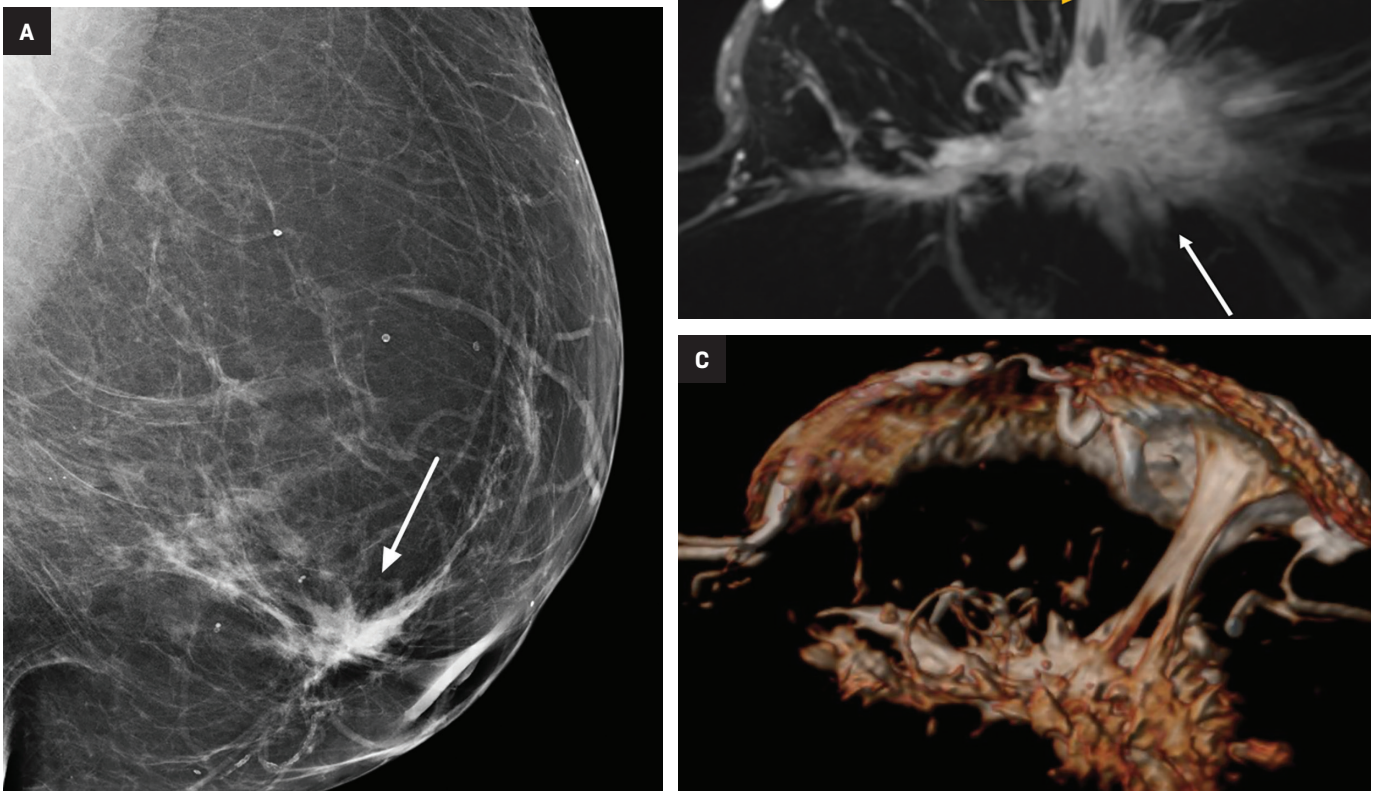
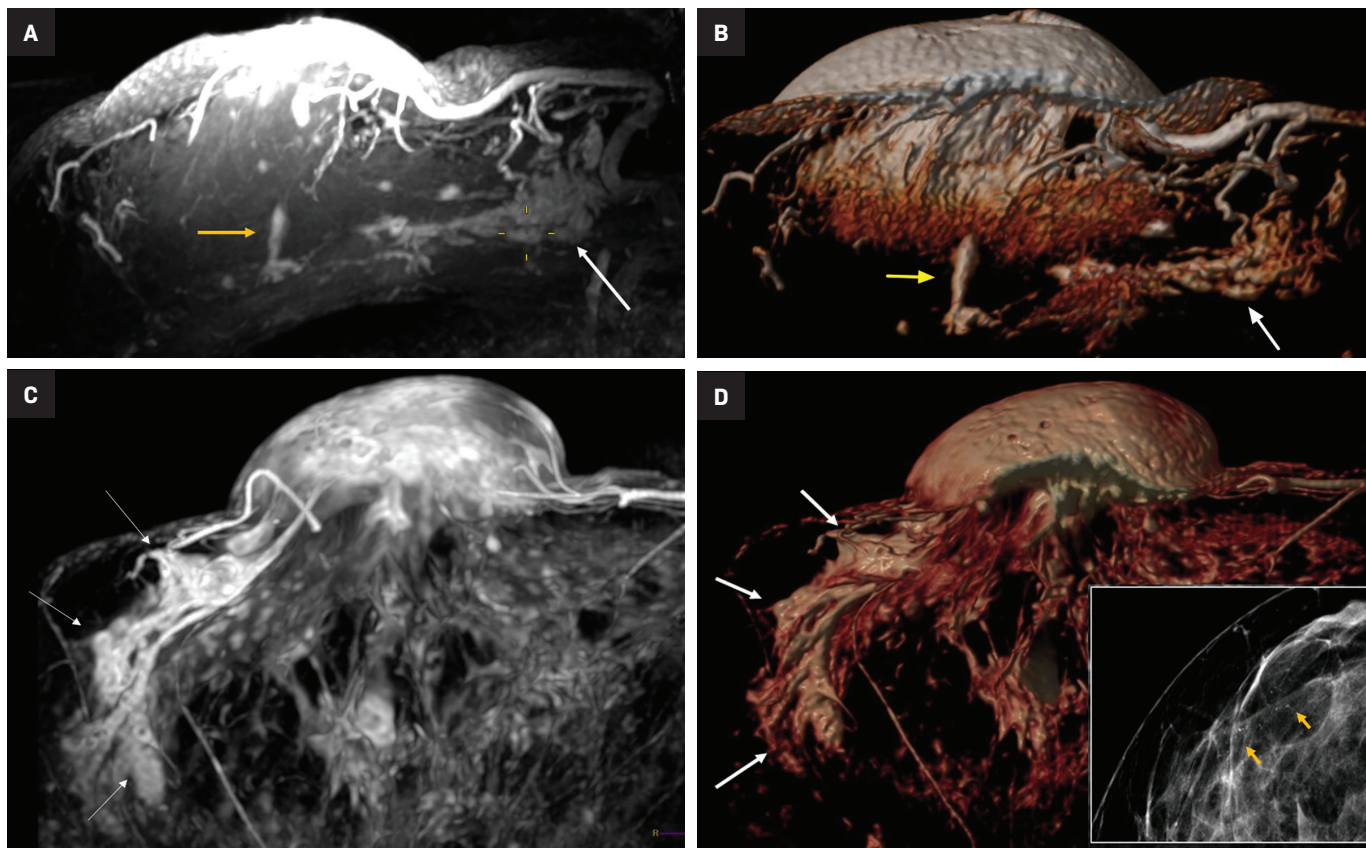




**Figure 11.** Two patients with Paget disease. Patient 1: eczema-like lesion on the nipple and serous discharge. (A) Axial T1 MIP with gadolinium and (B) volume rendering both showing segmental, non-mass enhancement (white arrow) confluent to a central duct facing the nipple (yellow arrow). Patient 2: (C) Axial T1 MIP with gadolinium and (D) volume rendering both showing an enlarged nipple and lateral segmental non-mass enhancement with nipple-oriented conglomerated rings (white arrows). (Inset: mammogram with punctate segmental macrocalcifications in a ductal adenocarcinoma [yellow arrows]).



14) Chen L, Zhou WB, Zhao Y, et al. Bloody nipple discharge is a predictor of breast cancer risk: a meta-analysis. *Breast Cancer Res Treat.* 2012;132(1): 9-14.

15) Tot T, Tabar L, Dean P. *Practical Breast Pathology 2014 2nd edition.* Thieme Verlag Gruppe, Stuttgart. Nueva York, 2014:86-93

16) Kim TH, Kang DK, Kim SY, Lee EJ, Jung YS y Yim H. Sonographic differentiation of benign and malignant papillary lesions of the breast. *J Ultrasound Med.* 2008; 27:75-82.

17) Son EJ, Kim EK, Kim JA, Kwak JY, Jeong J. Diagnostic value of 3D fast low-angle shot dynamic MRI of breast papillomas. *Yonsei Med J.* 2009; 50(6):838-44.

18) Ueng SH, Mezzetti T, Tavassoli FA. Papillary neoplasms of the breast: a review. *Arch Pathol Lab Med.* 2009; 133(6): 893-907.

19) Liberman L, Tornos C, Huzjan R, Bartella L, Morris EA, Dershaw DD. Is surgical excision warranted after benign, ¿concordant diagnosis of papilloma at percutaneous breast biopsy? *AJR Am J Roentgenol.* 2006; 186(5):1328-1334.

20) Li X, Aho M, Newell MS, et al. Papilloma diagnosed on core biopsies has a low upgrade rate. *Clin Imaging.* 2020; 60(1):67-74.

21) Tabár L, Tot T, Dean P. Understanding the breast in health and disease. Hong Kong. C & C Offset Printing Co. 2012; 7-9

22) Ramsay D, Kent J, Hartmann R, Hartmann P. Anatomy of the lactating human breast redefined with ultrasound imaging. *J Anat.* 2005; 206(6): 525-534.

23) Tabár L, Tot T, Dean P. Multimodality Imaging in the Interdisciplinary Management of Breast Diseases. In: Jones G, *Bostwick's Plastic and Reconstructive Breast Surgery, 4th Ed, Vol 1: Thieme;* 2020:119-134.

24) Tabár L, Tot T, Dean P. *Understanding the breast in health and disease.* Hong Kong. C & C Offset Printing Co; 2012:7-9.

25) Tot T, Gere M. Radiological-pathological correlation in diagnosing breast carcinoma: The role of pathology in the multimodality era. *Pathol Oncol Res.* 2008; 14(2):173-178.

26) Tot T, Gere M, Pekar G, Tarjan M, Hofmeyer S, Hellberg D, et al. Breast cancer multifocality, disease extent, and survival. *Hum Path.* 2011; 42(11):1761-1769.

27) Nakahara H, Namba K, Watanabe R. A comparison of MR imaging, galactography and ultrasonography in patients with nipple discharge. *Breast Cancer.* 2003;(4):320-329.

28) Lee Su Ju, Sobel L, Shamis M, Mahoney M. Asymmetric ductal ectasia: An often-overlooked sign of malignancy. *Am J Radiol.* 2019; 213(2):473-481.

29) Tozaki M, Igarashi T, Fukuda K. Breast MRI using the VIBE sequence: clustered ring enhancement in the differential diagnosis of lesions showing non-masslike enhancement. *Am J Radiol.* 2006; 187(2):313-321.

30) Tokuda Y, Kuriyama K, Nakamoto A, Choi S, Yutani K, Kunitomi Y, et al. Evaluation of suspicious nipple discharge by magnetic resonance mammography based on breast imaging reporting and data system magnetic resonance imaging descriptors. *J Comput Assist Tomogr.* 2009; 33:58-62

31) Sripathi S, Ayachit A, Kadavigere R, Kumar S, Eleti A, Sraj A. Spectrum of imaging findings in Paget's disease of the breast—a pictorial review. *Insights Imaging.* 2015; 6(4): 419-429.